*Article*

# Axial Stress-Strain Performance of Recycled Aggregate Concrete Reinforced with Macro-Polypropylene Fibres

Muhammad Junaid Munir [1,2,†] , Syed Minhaj Saleem Kazmi [1,2,†] , Yu-Fei Wu [1,2,*] , Xiaoshan Lin [2] and Muhammad Riaz Ahmad [3]

1   Guangdong Provincial Key Laboratory of Durability for Marine Civil Engineering, Shenzhen University, Shenzhen 518060, China; muhammad.munir@rmit.edu.au (M.J.M.); syed.kazmi@rmit.edu.au (S.M.S.K.)
2   School of Engineering, RMIT University, 376-392 Swanston St, Melbourne, VIC 3001, Australia; susanna.lin@rmit.edu.au
3   Department of Civil and Environmental Engineering, The Hong Kong Polytechnic University, Hung Hom, Kowloon, Hong Kong 999077, China; mriaz.ahmad@polyu.edu.hk
*   Correspondence: yufei.wu@szu.edu.cn
†   Joint First Author.

**Abstract:** The addition of macro-polypropylene fibres improves the stress-strain performance of natural aggregate concrete (NAC). However, limited studies focus on the stress-strain performance of macro-polypropylene fibre-reinforced recycled aggregate concrete (RAC). Considering the variability of coarse recycled aggregates (CRA), more studies are needed to investigate the stress-strain performance of macro-polypropylene fibre-reinforced RAC. In this study, a new type of 48 mm long BarChip macro-polypropylene fibre with a continuously embossed surface texture is used to produce BarChip fibre-reinforced NAC (BFNAC) and RAC (BFRAC). The stress-strain performance of BFNAC and BFRAC is studied for varying dosages of BarChip fibres. Results show that the increase in energy dissipation capacity (i.e., area under the curve), peak stress, and peak strain of samples is observed with an increase in fibre dosage, indicating the positive effect of fibre addition on the stress-strain performance of concrete. The strength enhancement due to the addition of fibres is higher for BFRAC samples than BFNAC samples. The reduction in peak stress, ultimate strain, toughness and specific toughness of concrete samples due to the utilisation of CRA also reduces with the addition of fibres. Hence, the negative effect of CRA on the properties of concrete samples can be minimised by adding BarChip macro-polypropylene fibres. The applicability of the stress-strain model previously developed for macro-synthetic and steel fibre-reinforced NAC and RAC to BFNAC and BFRAC is also examined.

**Keywords:** axial stress-strain performance; macro-polypropylene fibres; fibre-reinforced concrete; recycled aggregate concrete

## 1. Background

Concrete is the most widely used construction material globally, which is attributed to the availability of raw materials, low cost, and excellent performance [1,2]. To further improve the properties, various types of fibres are used in concrete [3–5]. The addition of fibres in concrete develops the stress transfer mechanism by bridging the cracks of samples after failure [6]. This mechanism improves the crack resisting ability and can help avoid the brittle failure of concrete samples [7]. Fibre-reinforced concrete (FRC) shows improved flexural strength, tensile strength, creep behaviour, ductility and post-cracking properties compared to conventional concrete and results in structural safety [8–10]. In the past few decades, FRC has been used widely for various non-structural and structural applications, including tunnel linings, precast elements, ground slabs, and pavements [11–13].

Various types of fibres are used to produce FRC. Generally, fibres are classified as steel, synthetic, glass and natural fibres [3–5]. Among all these fibres, steel fibres are

most commonly used to produced FRC owing to their excellent structural properties [14]. However, the durability properties, particularly the corrosion of steel FRC is a significant drawback, which increases the importance of other types of fibres [6]. The utilisation of synthetic fibres, such as polypropylene fibres, to produce FRC has increased rapidly in the past few years [7,15]. Polypropylene is a low cost and inert material that makes the polypropylene FRC cost-effective and durable [7]. Moreover, improved fracture toughness, impact resistance, ductility, tensile and bending capacity are leading to an increase in applications of polypropylene FRC [7,16,17]. Polypropylene fibres also increase thermal stability and improve the properties of concrete samples exposed to elevated temperatures [18–20]. Fibres are divided into two categories by their size, specifically, micro and macro fibres. Micro-fibres range from 6–20 mm in length and have a diameter of tens of microns, whereas macro-fibres range from 30–60 mm in length and have a diameter of more than 0.3 mm [21]. Micro-fibres are mostly used to control plastic shrinkage and have a limited contribution to the structural performance of FRC [21]. However, macro-fibres are quite useful in enhancing the structural performance of FRC, especially in a post-cracking scenario [22].

In the past few decades, the generation of concrete related waste has increased alarmingly due to the demolition of old buildings/structures [23,24]. As a result, there is a high demand for recycling the concrete waste generated in the production of new concrete [25,26]. The manufacturing and utilisation of recycled aggregate concrete (RAC) can solve a variety of issues, including natural resource depletion, landfill demand and related environmental pollution [1,27]. However, the low performance of RAC is a significant hurdle in the recycling of concrete waste, which is due to the weak and porous adhered mortar of recycled aggregates [28,29]. Therefore, the utilisation of RAC for new construction activities is quite limited [30]. Around a 20% reduction in compressive strength was observed for RAC compared to traditional concrete [31]. Likewise, decreases of 40 and 10% in the modulus of elasticity and tensile strength was reported for RAC compared to natural aggregate concrete (NAC) in past studies [32,33].

Many researchers are working to improve the performance of RAC [34–36]. In this context, various techniques, including pre-soaking in acid, mechanical grinding, pre-soaking in water, pozzolan slurry, heat grinding, polymer emulsion, carbonation, and calcium carbonate bio deposition, were used to enhance the performance of RAC [37–42]. A variety of fibres were also used to improve the deformation, bending, compressive, ductility, toughness, impact, and fatigue performance of RAC [43–48]. Steel fibre-reinforced RAC with 25% coarse natural aggregates (CNA) replaced with coarse recycled aggregates (CRA) showed a 13% rise in compressive strength for a 0.75% steel fibre dosage [45]. Likewise, polypropylene fibre-reinforced RAC with 55% CNA replaced with CRA showed 4 and 31% increases in flexural and tensile strengths, respectively, for a 1% polypropylene fibre dosage [49]. The number of fibres also strongly influences the residual flexural tensile strength (an important parameter to describe the post-cracking behaviour of fibre-reinforced concrete through the crack mouth opening displacement test) and fracture energy of RAC [7]. FRC incorporating macro-polypropylene fibres has no considerable effect on the compressive strength of concrete [50,51]. However, the other properties, including elastic modulus, toughness and strain of concrete, are influenced by the addition of macro-polypropylene fibres.

## 2. Significance

The application of macro-polypropylene fibres in normal concrete has been attracting attention from the construction industry due to their better performance than other fibres in terms of better distribution in concrete, lower weight, higher impact resistance and flexural strength, improved economy and better corrosion resistance [7,52]. Major areas of applications for macro synthetic fibres are tunnel linings, industrial floors and pavements, etc. [53]. Despite all the advantages of macro-polypropylene fibres and the availability of various studies in the literature related to the stress-strain performance of

macro-polypropylene fibre-reinforced NAC, very limited studies focus on the stress-strain performance of macro-polypropylene fibre-reinforced RAC [6]. Furthermore, considering the variability of CRA, more studies are needed to investigate the stress-strain performance of macro-polypropylene fibre-reinforced RAC. Therefore, in this study, a new type of 48 mm long BarChip macro-polypropylene fibre with continuously embossed surface texture is used to produce BarChip fibre-reinforced NAC (BFNAC) and RAC (BFRAC). This new type of continuously embossed surface fibre develops a stronger fibre-cement paste bond compared to fibres with straight surfaces leading to a more compact concrete structure [54]. The stress-strain behaviour of BFNAC and BFRAC is studied for varying dosages of BarChip fibres. The applicability of the stress-strain model previously developed for macro-synthetic and steel fibre-reinforced NAC and RAC to BFNAC and BFRAC is also examined.

## 3. Experimental Scheme

### 3.1. Materials and Preparation of Samples

In this work, 48 mm long BarChip macro-polypropylene fibres with a continuously embossed surface texture, as shown in Figure 1, are used to produce BFNAC and BFRAC. Table 1 presents the properties of BarChip macro-polypropylene fibres.



**Figure 1.** Barchip macro-polypropylene fibres.

**Table 1.** Properties of BarChip macro-polypropylene fibres.

| Base Material | Modified Olefin |
|---|---|
| Surface texture | Continuously embossed |
| Young modulus (GPa) | 10 |
| Eq. diameter (mm) | 0.65 |
| Specific gravity | 0.91 |
| Length (mm) | 48 |
| Tensile strength (MPa) | 640 |

To produce BFNAC and BFRAC, tap water, ordinary Portland cement, and natural river sand were used. Crushed basalt was used as NCA with a maximum size of 14 mm. Similarly, CRA of a maximum 14 mm size were obtained from a construction and demolition waste recycling plant. CRA are referred to as class 1B with impurities (ceramics, glass, asphalt and bricks) less than 10% [28,55]. The gradation of coarse aggregates (CA) is presented in Figure 2. The grading of both CA is quite close and follows the criteria of AS 2758.1:2014 [56]. Properties of CA are also presented in Table 2, where the higher water absorption of CRA compared to CNA shows the inferior performance of CRA.
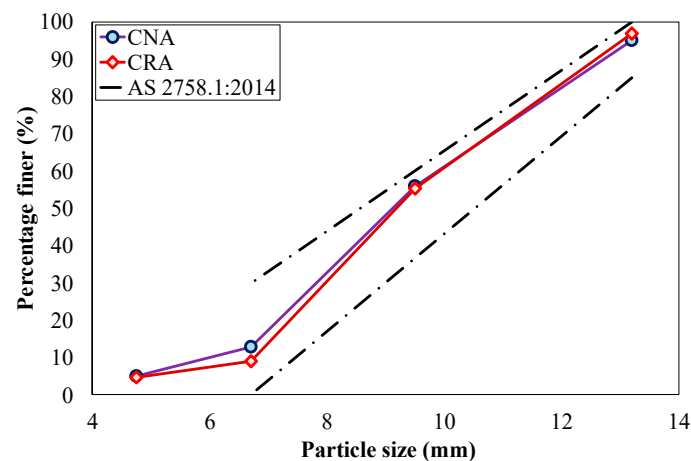
**Figure 2.** Gradation of CA.

**Table 2.** Properties of CA.

| Type of CA | Water Absorption (%) | Bulk Density (kg/m$^3$) | Specific Gravity |
|:---:|:---:|:---:|:---:|
| CNA | 2.06 | 1512 | 2.53 |
| CRA | 7.61 | 1413 | 2.32 |

Table 3 presents the details of concrete mixtures. All the concrete mixes were prepared following ASTM C192:2016 [57] guidelines. In this study, three different fibre dosages (i.e., 0, 0.5 and 1% of the concrete volume) were used. All the aggregates were dried in the oven, and then additional water was added to each concrete mix to compensate for the water absorption of aggregates, similar to previous studies [6,52,58]. For each mix, three samples of size 150 × 300 mm were prepared and tested, and results are reported as an average. Concrete samples were designated to represent the concrete type (NC and RC show NAC and RAC, respectively) and the dosage of BarChip macro-polypropylene fibres (B0.5 and B1 show 0.5 and 1% fibre dosage, respectively). For instance, RC-B0.5 samples represent the BFRAC samples reinforced with a 0.5% dosage of BarChip fibres. A drop in the workability/slump of concrete was observed with the increase in fibre dosage (Table 3).

**Table 3.** Details of concrete mixtures.

| Group | CNA (kg/m$^3$) | CRA (kg/m$^3$) | Sand (kg/m$^3$) | Water (kg/m$^3$) | Fibres (%) | Cement (kg/m$^3$) | Additional Water (kg/m$^3$) | Slump (mm) |
|:---:|:---:|:---:|:---:|:---:|:---:|:---:|:---:|:---:|
| NC | 822 | - | | | - | | 17 | 50 |
| NC-B0.5 | 822 | - | | | 0.5 | | 17 | 30 |
| NC-B1 | 822 | - | 709 | 185 | 1.0 | 451 | 17 | 10 |
| RC | - | 822 | | | - | | 63 | 60 |
| RC-B0.5 | - | 822 | | | 0.5 | | 63 | 40 |
| RC-B1 | - | 822 | | | 1.0 | | 63 | 30 |

*3.2. Test Plan*

In the beginning, all the concrete samples were compressed to 30% of their peak load three times following past studies [6,59] to remove the slackness of the system and eccentricity of loading. For measuring the stress-strain performance, the concrete samples were compressed through a compression testing machine of 1000 kN capacity under displacement control mode of 0.3 mm/min, and the applied load was recorded through a data acquisition system. The deformation of concrete samples was measured in this study through two linear variable displacement transducers (LVDTs) placed at 180° to each other.

## 4. Results and Discussion

### 4.1. General Behaviour

Figure 3 presents the failed concrete samples after the compression test. NC samples show smaller sized cracks in larger numbers compared to RC samples, which are related to the lower ductility and energy dissipation capacity of RC samples compared to NC samples [1,60]. During the compression testing, RC samples also show more brittle behaviour than NC samples due to the weak bond of CRA with the cement paste [34,61]. The failure pattern of concrete samples without fibres changes from a single large crack to a group of small cracks after the addition of fibres [6]. For BFNAC and BFRAC samples, fibres control the cracking and result in higher ultimate capacity and ductility of samples. All the BFNAC and BFRAC samples show minor cracks on the surface owing to the arresting of crack growth by the fibres. This phenomenon is observed to be more prominent for NC-B1 and RC-B1 samples than for NC-B0.5 and RC-B0.5 samples, respectively. BFNAC and BFRAC samples sustain the load and show large deformation without crushing into pieces. The failure pattern of BFNAC and BFRAC samples is observed to be quite similar, which shows the effectiveness of fibres to control the brittle nature of RC samples.
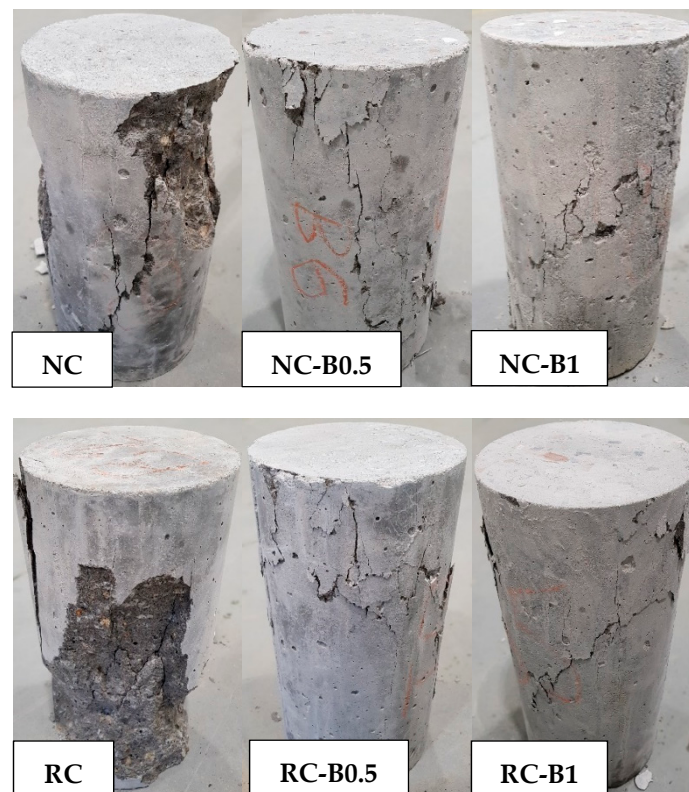


**Figure 3.** Concrete samples after compression test.

### 4.2. Axial Stress-Strain Behaviour

Figure 4 shows the stress-strain behaviour of NAC and RAC samples for different fibre dosages. The axial strain of concrete samples was measured in this study through an average displacement of two LVDTs placed at 180° to each other. Due to the relative movement between test machine platens, the slackness of the measurement system and loading, along with the deformability of any type of capping at the end of the sample, LVDT measurement systems show higher displacement values than the actual values [62]. To minimise this error, both sides of the samples were first ground and then samples were pre-compressed to 30% of their peak load three times, following past studies [5,41], before compression testing.
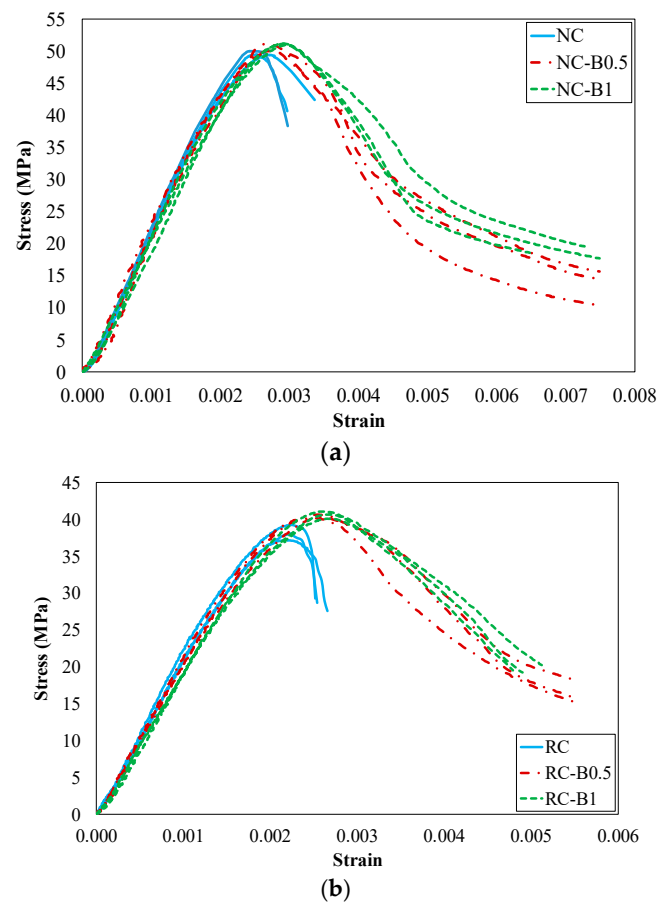
**Figure 4.** Stress-strain performance of concrete samples for different fibre dosages: (**a**) NAC samples and (**b**) RAC samples.

Figure 4 shows the increase in energy dissipation capacity (i.e., area under the curve), peak stress and peak strain of samples with an increase in fibre dosage, indicating the positive effect of fibre addition on concrete. The strength enhancement due to the addition of fibres is higher for RC samples than NC samples, according to the conclusions reported by Nataraja et al. [63] that fibre addition more prominently affects the low-strength concrete than high-strength concrete.

The stress-strain performance of all the concrete samples for different CA is presented in Figure 5. Lower stress-strain curves are observed for concrete samples with CRA than samples with CNA. A lower peak strength along with a lower elastic modulus (i.e., the smaller initial slope of the stress-strain curve) is observed for all the RAC samples compared to NAC samples. RC samples also show a steeper and shorter descending part of the stress-strain curve than NC samples, which is related to the more brittle characteristics of the RC samples compared to the NC samples, similarly to past studies [58,64,65]. Moreover, the area under the curve, i.e., energy absorption capacity, is also lower for RC samples compared to NC samples. However, no such behaviour is observed for BFRAC samples compared to BFNAC samples. The reduction in strength due to CRA is also observed relatively lower for RC-B0.5 and RCB1 samples compared to the RC samples, similarly to a past study [66].
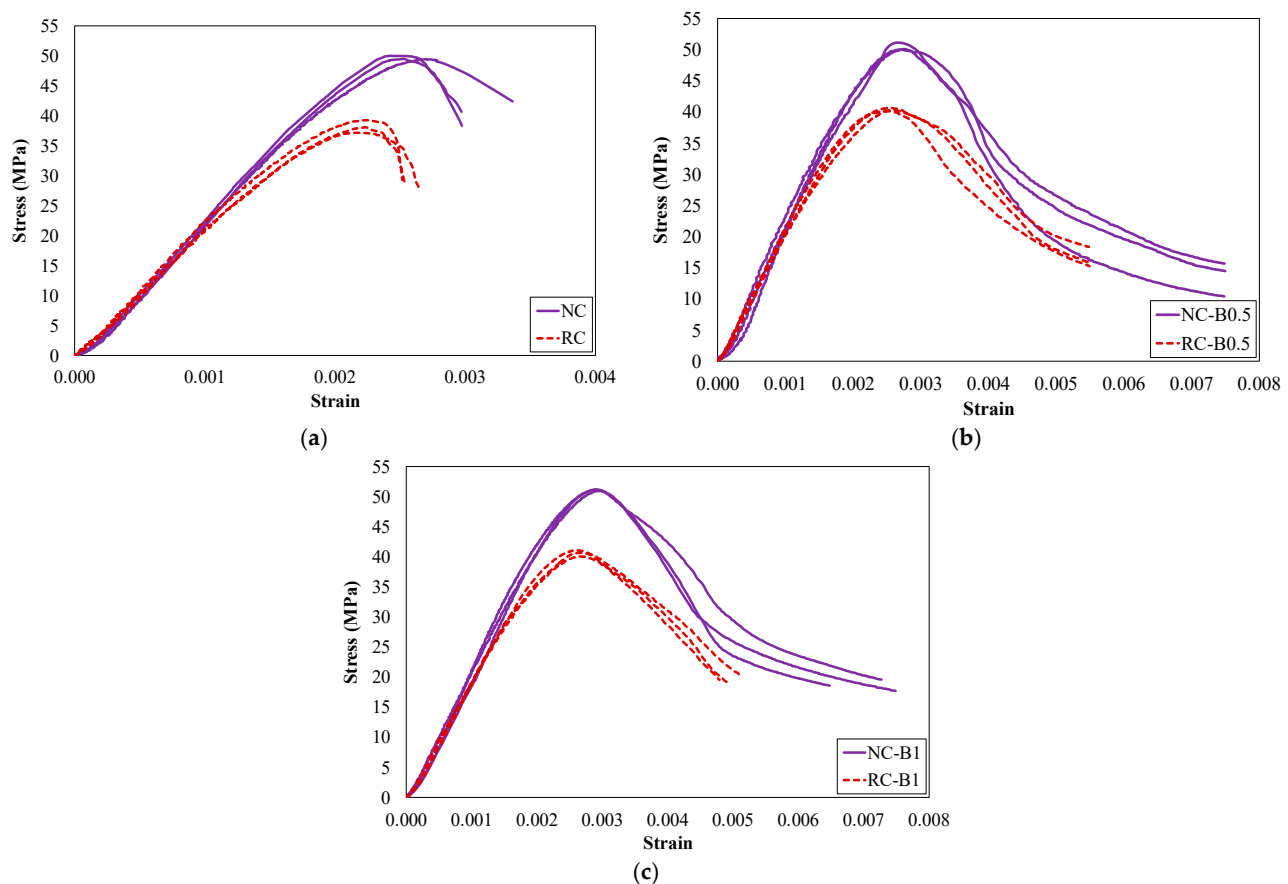
**Figure 5.** Stress-strain performance of concrete samples for different CA: (**a**) unreinforced samples, (**b**) BFNAC and BFRAC samples with 0.5% fibre dosage, (**c**) BFNAC and BFRAC samples with a 1% fibre dosage.
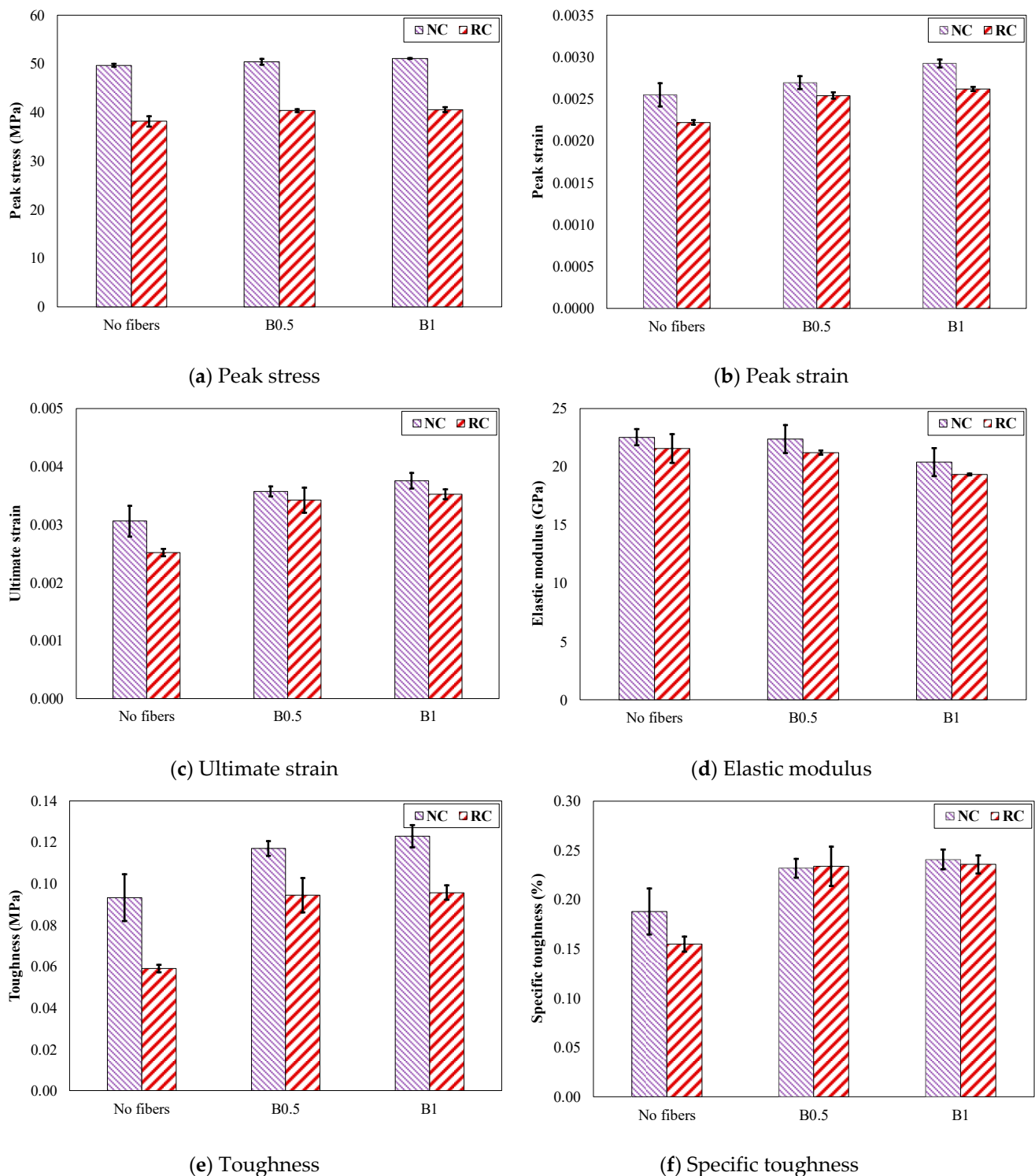
*4.3. Stress-Strain Properties*

4.3.1. Peak Stress

Figure 6a presents the peak stress of BFNAC and BFRAC samples. NC samples show a peak stress of 50 MPa, which reduces to 38 MPa for RC samples. However, increased peak stress of concrete samples is observed with an increase in fibre dosage. NC-B1 and RC-B1 samples show peak stress 3 and 6% higher than NC and RC samples, respectively. The fibre addition reduces the wing-crack growth rate by resisting the development of micro-cracks and results in the improved mechanical performance of concrete samples [67]. Still, the peak stress of RC-B0.5 and RC-B1 samples is lower than the NC samples.

RC samples show peak stress 23% lower than NC samples. Previously, Kou et al. [68] also reported a 26% lower peak stress of RAC samples than NAC samples. Comparing RC with NC and RC-B1 with NC-B1, the reduction in strength due to CRA reduces from 23% to 21%. Hence, the negative effect of CRA on the properties of concrete samples can be slightly reduced (up to 2%) by adding BarChip macro-polypropylene fibres. In a past study [66], similar behaviour was observed for steel fibre-reinforced RAC.

4.3.2. Peak Strain

Figure 6b presents the peak strain of BFNAC and BFRAC samples. NC samples show a peak strain of 0.0025, which reduces to 0.0022 for RC samples. However, an increased peak strain of concrete samples is noticed with an increase in fibre dosage. NC-B1 and RC-B1 samples show peak strain 15 and 18% higher than NC and RC samples, respectively. The peak strain of all the FRC samples is higher than the NC samples.

(**a**) Peak stress

(**b**) Peak strain

(**c**) Ultimate strain

(**d**) Elastic modulus

(**e**) Toughness

(**f**) Specific toughness

**Figure 6.** Stress-strain properties of BFNAC and BFRAC samples: (**a**) peak stress, (**b**) peak strain, (**c**) ultimate strain, (**d**) elastic modulus, (**e**) toughness, (**f**) specific toughness.

All the RAC samples have peak strain lower than respective NAC samples. Previously, the peak strain of RAC samples was observed to be higher compared to NAC samples [69]. However, the opposite trend is noticed in this study, which is related to the elastic modulus of samples similar to a previous study [1]. A higher drop in the modulus of elasticity results in higher deformation and higher peak strain. For example, Xiao et al. [70] reported a 45% higher drop in the modulus of elasticity for RAC samples compared to NAC samples, which

resulted in larger deformation and a 20% increase in the peak strain of RAC compared to NAC. However, RC samples show only a 4% decrease in elastic modulus than NC samples in this study, which results in a lower peak strain of RC samples (i.e., lesser than NC samples).

### 4.3.3. Ultimate Strain

Figure 6c presents the ultimate strain of BFNAC and BFRAC samples, which is determined at 85% of peak strength following past studies [1,60]. NC samples show an ultimate strain of 0.0031, which reduces to 0.0025 for RC samples. However, an increased ultimate strain of concrete samples is observed with an increase in fibre dosage. NC-B1 and RC-B1 samples show an ultimate strain that is 23 and 40% higher than NC and RC samples, respectively. The ultimate strain of all the FRC samples is higher than the NC samples. Comparing RC with NC and RC-B1 with NC-B1, the reduction in ultimate strain due to CRA decreases from 18% to 6%. Hence, the negative effect of CRA on the ultimate strain of samples can be minimised by adding BarChip macro-polypropylene fibres. In a past study [45], similar behaviour is observed for steel fibre-reinforced RAC.

### 4.3.4. Elastic Modulus

Figure 6d presents the modulus of elasticity of BFNAC and BFRAC samples, which is calculated following past studies [6,60]. NC samples have a modulus of elasticity of 23 GPa, which decreases to 22 GPa for RC samples. The low elastic modulus of RC samples comparer to NC samples is related to inferior RCA performance compared to NCA [70,71]. Previously, 45% decreased elastic modulus of RAC compared to NAC is reported by Xiao et al. [70]. Decreased modulus of elasticity of concrete samples is also noticed with an increase in fibre dosage. NC-B1 and RC-B1 samples show elastic modulus 9 and 10% lower than NC and RC samples, respectively. The elastic modulus of all the concrete samples is lower than the NC samples. In a previous study, Suksawang et al. [72] also reported the reduced elastic modulus of concrete samples reinforced with a variety of fibres. Generally, the addition of BarChip macro-polypropylene fibres should not influence the elastic modulus of samples. Therefore, the reduced elastic modulus of BFNAC and BFRAC samples is due to the influence of the fibre addition on the compaction/consolidation of concrete samples [72]. Moreover, the elastic modulus of concrete samples is also affected by the fibres in the direction parallel to the application of load being acting as voids [14].

### 4.3.5. Toughness

Figure 6e presents the toughness of BFNAC and BFRAC samples, which is calculated following past studies [6,60]. NC samples show a toughness of 0.09 MPa, which reduces to 0.06 MPa for RC samples. The reduced toughness of RAC samples compared to NAC samples is due to the lower peak stress of RAC samples than NAC samples [73]. However, increased toughness of concrete samples is observed with an increase in fibre dosage. NC-B1 and RC-B1 samples show toughness 32 and 62% higher than NC and RC samples, respectively. The toughness of all the BFNAC and BFRAC samples is higher than the NC samples. Comparing RC with NC and RC-B1 with NC-B1, the reduction in toughness due to CRA reduces from 37% to 22%. Hence, the negative effect of CRA on the properties of concrete samples can be minimised by adding BarChip macro-polypropylene fibres.

### 4.3.6. Specific Toughness

The specific toughness of concrete in compression is the ratio of the area under the stress-strain curve to the compressive strength of the concrete cylinder [74,75]. Figure 6f presents the specific toughness of BFNAC and BFRAC samples, which is calculated following past studies [6,60]. NC samples show the specific toughness of 0.19%, which reduces to 0.15% for RC samples. However, increased specific toughness of concrete samples is observed with an increase in fibre dosage. NC-B1 and RC-B1 samples show specific toughness 28 and 52% higher than NC and RC samples, respectively. The specific toughness of

all the BFNAC and BFRAC samples is higher than the NC samples. Comparing RC with NC and RC-B1 with NC-B1, the reduction in specific toughness due to CRA reduces from 18% to 2%, similar to a past study [43]. Hence, the negative effect of CRA on the specific toughness of concrete samples can be minimised by adding BarChip macro-polypropylene fibres.

### 4.4. Analytical Modelling

Recently, Kazmi et al. [5] developed a model to predict the axial stress-strain behaviour of steel and macro-synthetic fibre-reinforced RAC and NAC, considering an extensive test database. Equations (1)–(5) present the Kazmi et al. [5] stress-strain model for predicting the behaviour of macro-synthetic fibre-reinforced NAC and RAC.

$$f_c = (f_{cf} \cdot x \cdot \beta)/(\beta - 1 + x^\beta) \tag{1}$$

where

$$x = \varepsilon_c/\varepsilon_{cf} \tag{2}$$

$$\beta = 5.65(RI)^{0.3} + 0.14R \tag{3}$$

$$f_{cf} = f_c{}' + (1.96 + 0.8(R)^{0.18})RI \tag{4}$$

$$\varepsilon_{cf} = \varepsilon_c{}' + (0.00054 + 0.000008(R)^{8.5})RI \tag{5}$$

where $f_c$ and $\varepsilon_c$ are the axial stress and axial strain at any point of the stress-strain curve, respectively; $f_c{}'$ and $f_{cf}$ are the peak stresses of unreinforced and macro-polypropylene fibre-reinforced concrete samples, respectively; $\varepsilon_c{}'$ and $\varepsilon_{cf}$ are the peak strains of unreinforced and macro-polypropylene fibre-reinforced concrete samples, respectively; $R$ is the CRA replacement ratio ranges from 0–1 (which is equal to 0 for 0% CRA replacement ratio and 1 for 100% CRA replacement ratio); $RI$ is the reinforcing index determined by multiplying the aspect ratio with the volume of fibres. The Kazmi et al. [6] model is applicable for $RI$ from 0.08–0.88, $f_c{}'$ from 28–54 MPa, CRA replacement ratio from 0–100% and wavy, embossed and smooth texture of macro-polypropylene fibres.

The applicability of the stress-strain model developed by Kazmi et al. [6] for macro-synthetic and steel fibre-reinforced NAC and RAC to BFNAC and BFRAC is examined in this work. The performance of the Kazmi et al. [6] model to predict the stress-strain relationships of BFNAC and BFRAC samples is presented in Figure 7. The predicted results are evaluated through an error index [6]:

$$Error\ index = \sum (\,|\,R_{Exp.} - R_{Ana.}\,|\,/R_{Exp.})/N \tag{6}$$

where $N$ is the number of BFNAC and BFRAC samples considered in this study; $R_{Ana.}$ and $R_{Exp.}$ are predicted and measured results of BFNAC and BFRAC samples, respectively.
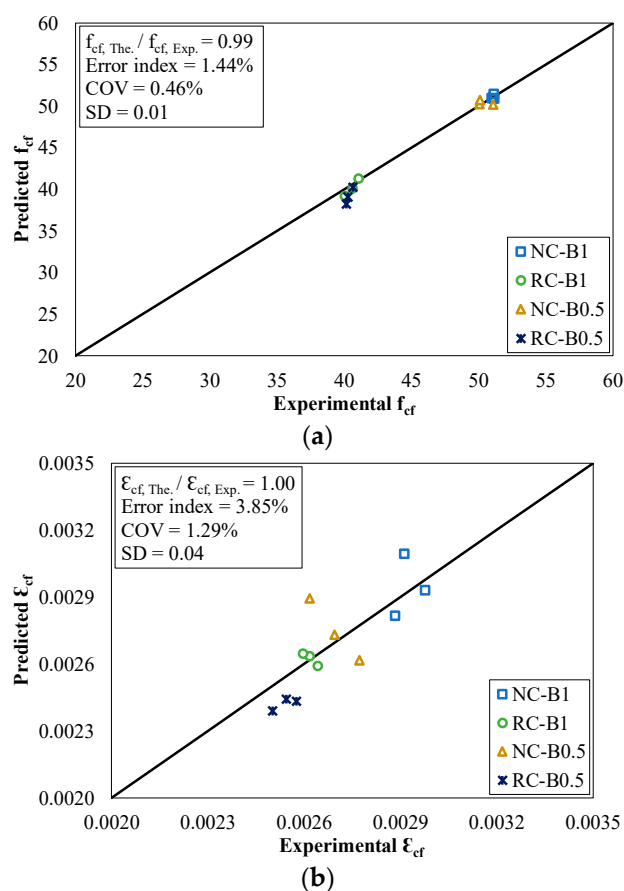
(a)



(b)

**Figure 7.** Evaluation of the Kazmi et al. [5] model to predict the (**a**) peak stress and (**b**) peak strain of BFNAC and BFRAC samples.

The predicted values of peak stress and peak strain are close to the measured results of BFNAC and BFRAC samples by an error index of 1 and 4%, respectively. Figure 8 presents the prediction of the axial stress-strain performance of BFNAC and BFRAC samples by the Kazmi et al. [6] model. The experimental curves are observed quite close to the predicted curves. Therefore, the Kazmi et al. [6] model can effectively predict the axial stress-strain behaviour of BFNAC and BFRAC samples.
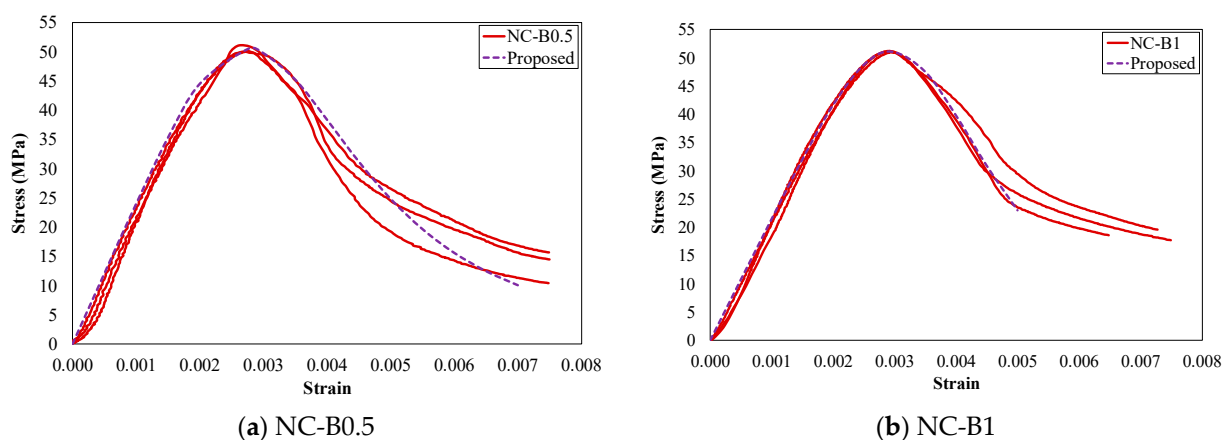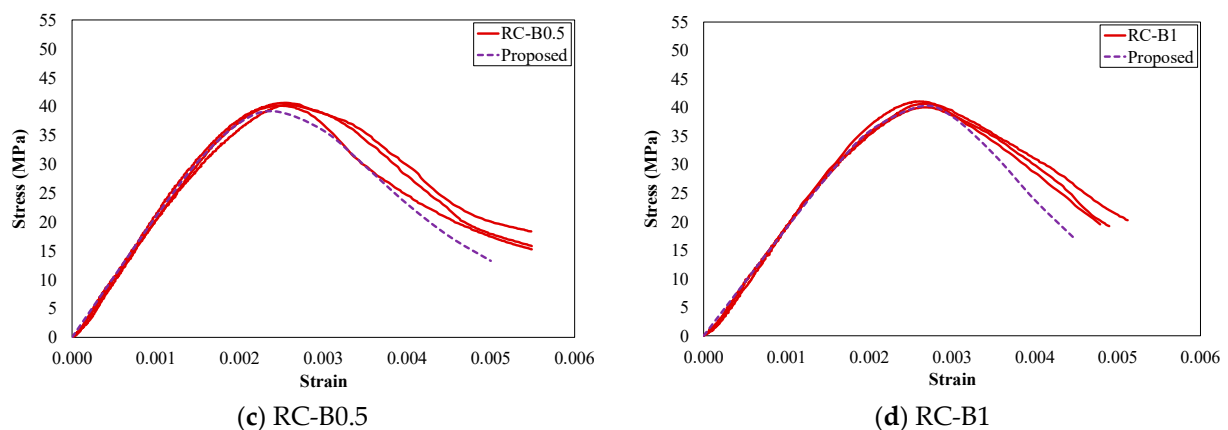


(**a**) NC-B0.5



(**b**) NC-B1

**Figure 8.** *Cont.*

**(c)** RC-B0.5            **(d)** RC-B1

**Figure 8.** Prediction of the axial stress-strain performance of BFNAC and BFRAC samples by the Kazmi et al. [6] model:
(**a**) NC-B0.5, (**b**) NC-B1, (**c**) RC-B0.5, (**d**) RC-B1.

### *4.5. Effect of Fibre Type on the Axial Stress-Strain Behaviour*

The Kazmi et al. [6] model is applicable for the wavy, embossed and smooth texture of macro-polypropylene fibres with Young's modulus between 6–14 GPa and tensile strength between 320–660 MPa. The BarChip macro-polypropylene fibres considered in this study have an embossed texture with Young's modulus and tensile strength of 10 GPa and 640 MPa, respectively. Thus, the Kazmi et al. [6] model is suitable to predict the stress-strain performance of BFNAC and BFRAC samples. The mechanical properties of fibre-reinforced concrete are greatly affected by the fibre characteristics, including surface texture, Young's modulus and tensile strength [17,76]. Scant work is available in the literature focusing on the stress-strain performance of macro-polypropylene fibre-reinforced RAC and NAC, which is a major hurdle in establishing the effect of different types of macro polypropylene fibres on the axial stress-strain behaviour of concrete samples. Therefore, a detailed investigation to understand the effect of different types of macro-polypropylene fibres on the stress-strain performance of concrete is recommended for future research.

### 5. Summary and Conclusions

The following are the conclusions of this study:

- Increases in energy dissipation capacity (i.e., area under the curve), peak stress, and peak strain of samples are noticed with an increase in fibre dosage, indicating the positive effect of fibre addition on the stress-strain performance of concrete. Strength enhancement due to the addition of fibres is also noticed to be higher for RC samples than for NC samples.

- An increase of 3 and 6% in the peak stress is observed for the NC-B1 and RC-B1 samples, respectively. The fibre addition reduces the wing-crack growth rate by resisting the development of micro-cracks and results in the improved mechanical performance of concrete samples.

- NC samples show a peak strain of 0.0025, which reduces to 0.0022 for RC samples. However, an increased peak strain of concrete samples is noticed with an increase in fibre dosage. NC-B1 and RC-B1 samples show peak strain 15 and 18% higher than NC and RC samples, respectively. The peak strain of all the FRC samples is higher than the NC samples.

- NC samples show an ultimate strain of 0.0031, which reduces to 0.0025 for RC samples. However, an increased ultimate strain of concrete samples is observed with an increase in fibre dosage. NC-B1 and RC-B1 samples show an ultimate strain 23 and 40% higher than NC and RC samples, respectively. The ultimate strain of all the FRC samples is higher than the NC samples.

- NC samples have a modulus of elasticity of 23 GPa, which decreases to 22 GPa for RC samples. Decreased modulus of elasticity of concrete samples is also noticed with an increase in fibre dosage, which is due to the influence of the fibre addition on the compaction/consolidation of concrete samples. The elastic modulus of all the concrete samples is lower than the NC samples.
- NC samples show the specific toughness of 0.19%, which reduces to 0.15% for RC samples. However, increased specific toughness of concrete samples is observed with an increase in fibre dosage. NC-B1 and RC-B1 samples show specific toughness 28 and 52% higher than NC and RC samples, respectively. The specific toughness of all the BFNAC and BFRAC samples is higher than the NC samples. Hence, the negative effect of CRA on the properties of concrete samples can be minimised by adding BarChip macro-polypropylene fibres.
- The applicability of the stress-strain model developed by Kazmi et al. [5] for macro-synthetic and steel fibre-reinforced NAC and RAC to BFNAC and BFRAC is examined in this study. The predicted values of peak stress and peak strain are close to the measured results of BFNAC and BFRAC samples by an error index of 1 and 4%, respectively. The experimental stress-strain curves are also quite close to the predicted curves. Therefore, the Kazmi et al. [5] model can effectively predict the axial stress-strain behaviour of BFNAC and BFRAC samples.

## References

1. Munir, M.J.; Kazmi, S.M.S.; Wu, Y.-F.; Patnaikuni, I.; Wang, J.; Wang, Q. Development of a unified model to predict the axial stress–strain behavior of recycled aggregate concrete confined through spiral reinforcement. *Eng. Struct.* **2020**, *218*, 110851. [CrossRef]
2. Wu, Y.-F.; Kazmi, S.M.S.; Munir, M.J.; Zhou, Y.; Xing, F. Effect of compression casting method on the compressive strength, elastic modulus and microstructure of rubber concrete. *J. Clean. Prod.* **2020**, *264*, 121746. [CrossRef]
3. Fu, Q.; Niu, D.; Li, D.; Wang, Y.; Zhang, J.; Huang, D. Impact characterization and modelling of basalt-polypropylene fibre-reinforced concrete containing mineral admixtures. *Cem. Concr. Compos.* **2018**, *93*, 246–259. [CrossRef]
4. Afroughsabet, V.; Biolzi, L.; Monteiro, P.J.M. The effect of steel and polypropylene fibers on the chloride diffusivity and drying shrinkage of high-strength concrete. *Compos. Part B Eng.* **2018**, *139*, 84–96. [CrossRef]
5. Banyhussan, Q.S.; Yıldırım, G.; Bayraktar, E.; Demirhan, S.; Şahmaran, M. Deflection-hardening hybrid fiber reinforced concrete: The effect of aggregate content. *Constr. Build. Mater.* **2016**, *125*, 41–52. [CrossRef]
6. Kazmi, S.M.S.; Munir, M.J.; Wu, Y.-F.; Patnaikuni, I.; Zhou, Y.; Xing, F. Axial stress-strain behavior of macro-synthetic fiber reinforced recycled aggregate concrete. *Cem. Concr. Compos.* **2019**, *97*, 341–356. [CrossRef]
7. Kazmi, S.M.S.; Munir, M.J.; Wu, Y.-F.; Patnaikuni, I. Effect of macro-synthetic fibers on the fracture energy and mechanical behavior of recycled aggregate concrete. *Constr. Build. Mater.* **2018**, *189*, 857–868. [CrossRef]

8. Mudadu, A.; Tiberti, G.; Germano, F.; Plizzari, G.A.; Morbi, A. The effect of fiber orientation on the post-cracking behavior of steel fiber reinforced concrete under bending and uniaxial tensile tests. *Cem. Concr. Compos.* **2018**, *93*, 274–288. [CrossRef]

9. Song, Q.; Yu, R.; Shui, Z.; Rao, S.; Wang, X.; Sun, M.; Jiang, C. Steel fibre content and interconnection induced electrochemical corrosion of Ultra-High Performance Fibre Reinforced Concrete (UHPFRC). *Cem. Concr. Compos.* **2018**, *94*, 191–200. [CrossRef]

10. Teng, S.; Afroughsabet, V.; Ostertag, C.P. Flexural behavior and durability properties of high performance hybrid-fiber-reinforced concrete. *Constr. Build. Mater.* **2018**, *182*, 504–515. [CrossRef]

11. Afroughsabet, V.; Ozbakkaloglu, T. Mechanical and durability properties of high-strength concrete containing steel and polypropylene fibers. *Constr. Build. Mater.* **2015**, *94*, 73–82. [CrossRef]

12. Sahmaran, M.; Yurtseven, A.; Ozgur Yaman, I. Workability of hybrid fiber reinforced self-compacting concrete. *Build. Environ.* **2005**, *40*, 1672–1677. [CrossRef]

13. Sahmaran, M.; Yaman, I.O. Hybrid fiber reinforced self-compacting concrete with a high-volume coarse fly ash. *Constr. Build. Mater.* **2007**, *21*, 150–156. [CrossRef]

14. Neves, R.D.; Almeida, J.C.O.F.D. Compressive behaviour of steel fibre reinforced concrete. *Struct. Concr.* **2005**, *6*, 1–8. [CrossRef]

15. Amin, A.; Foster, S.J.; Gilbert, R.I.; Kaufmann, W. Material characterisation of macro synthetic fibre reinforced concrete. *Cem. Concr. Compos.* **2017**, *84*, 124–133. [CrossRef]

16. Das, C.S.; Dey, T.; Dandapat, R.; Mukharjee, B.B.; Kumar, J. Performance evaluation of polypropylene fibre reinforced recycled aggregate concrete. *Constr. Build. Mater.* **2018**, *189*, 649–659. [CrossRef]

17. Sadrinejad, I.; Madandoust, R.; Ranjbar, M.M. The mechanical and durability properties of concrete containing hybrid synthetic fibers. *Constr. Build. Mater.* **2018**, *178*, 72–82. [CrossRef]

18. Drzymała, T.; Jackiewicz-Rek, W.; Gałaj, J.; Šukys, R. Assessment of mechanical properties of high strength concrete (HSC) after exposure to high temperature. *J. Civ. Eng. Manag.* **2018**, *24*, 138–144. [CrossRef]

19. Rudnik, E.; Drzymała, T. Thermal behavior of polypropylene fiber-reinforced concrete at elevated temperatures. *J. Therm. Anal. Calorim.* **2018**, *131*, 1005–1015. [CrossRef]

20. Jackiewicz-Rek, W.; Drzymała, T.; Kuś, A.; Tomaszewski, M. Durability of high performance concrete (HPC) subject to fire temperature impact. *Arch. Civ. Eng.* **2016**, *62*, 73–93. [CrossRef]

21. Ahmed, W.; Lim, C.W. Production of sustainable and structural fiber reinforced recycled aggregate concrete with improved fracture properties: A review. *J. Clean. Prod.* **2021**, *279*, 123832. [CrossRef]

22. Kazmi, S.M.S.; Munir, M.J.; Wu, Y.-F.; Patnaikuni, I. Mechanical and post-cracking performance of recycled aggregate concrete incorporating synthetic fibers. *IOP Conf. Ser. Mater. Sci. Eng.* **2020**, *829*, 012003. [CrossRef]

23. Xu, F.; Wang, S.; Li, T.; Liu, B.; Li, B.; Zhou, Y. The mechanical properties of tailing recycled aggregate concrete and its resistance to the coupled deterioration of sulfate attack and wetting–drying cycles. *Structures* **2020**, *27*, 2208–2216. [CrossRef]

24. Bandyopadhyay, A.; Maurya, K.K.; Samanta, A.K. Investigation on UPVC confined RC columns with Recycled Aggregate Concrete using C&D waste. *Structures* **2020**, *23*, 279–288. [CrossRef]

25. Oikonomou, N.D. Recycled concrete aggregates. *Cem. Concr. Compos.* **2005**, *27*, 315–318. [CrossRef]

26. Kazmi, S.M.S.; Munir, M.J.; Wu, Y.-F.; Patnaikuni, I.; Zhou, Y.; Xing, F. Effect of different aggregate treatment techniques on the freeze-thaw and sulfate resistance of recycled aggregate concrete. *Cold Reg. Sci. Technol.* **2020**, *178*, 103126. [CrossRef]

27. Kazmi, S.M.S.; Munir, M.J.; Wu, Y.-F.; Patnaikuni, I.; Zhou, Y.; Xing, F. Effect of recycled aggregate treatment techniques on the durability of concrete: A comparative evaluation. *Constr. Build. Mater.* **2020**, *264*, 120284. [CrossRef]

28. Tam, V.W.Y. Comparing the implementation of concrete recycling in the Australian and Japanese construction industries. *J. Clean. Prod.* **2009**, *17*, 688–702. [CrossRef]

29. Kisku, N.; Rajhans, P.; Panda, S.K.; Pandey, V.; Nayak, S. Microstructural investigation of recycled aggregate concrete produced by adopting equal mortar volume method along with two stage mixing approach. *Structures* **2020**, *24*, 742–753. [CrossRef]

30. Kazmi, S.M.S.; Munir, M.J.; Wu, Y.-F. Application of waste tire rubber and recycled aggregates in concrete products: A new compression casting approach. *Resour. Conserv. Recycl.* **2021**, *167*, 105353. [CrossRef]

31. Xiao, J.; Li, W.; Fan, Y.; Huang, X. An overview of study on recycled aggregate concrete in China (1996–2011). *Constr. Build. Mater.* **2012**, *31*, 364–383. [CrossRef]

32. Kou, S.C.; Poon, C.S.; Chan, D. Influence of fly ash as cement replacement on the properties of recycled aggregate concrete. *J. Mater. Civ. Eng.* **2007**, *19*, 709–717. [CrossRef]

33. Kou, S.-C.; Poon, C.-S.; Etxeberria, M. Influence of recycled aggregates on long term mechanical properties and pore size distribution of concrete. *Cem. Concr. Compos.* **2011**, *33*, 286–291. [CrossRef]

34. Kim, Y.; Hanif, A.; Kazmi, S.M.S.; Munir, M.J.; Park, C. Properties enhancement of recycled aggregate concrete through pretreatment of coarse aggregates–Comparative assessment of assorted techniques. *J. Clean. Prod.* **2018**, *191*, 339–349. [CrossRef]

35. Kisku, N.; Joshi, H.; Ansari, M.; Panda, S.K.; Nayak, S.; Dutta, S.C. A critical review and assessment for usage of recycled aggregate as sustainable construction material. *Constr. Build. Mater.* **2017**, *131*, 721–740. [CrossRef]

36. Kazmi, S.M.S.; Munir, M.J.; Wu, Y.-F.; Lin, X.; Ahmad, M.R. Investigation of thermal performance of concrete incorporating different types of recycled coarse aggregates. *Constr. Build. Mater.* **2020**, *270*, 121433. [CrossRef]

37. Shi, C.; Li, Y.; Zhang, J.; Li, W.; Chong, L.; Xie, Z. Performance enhancement of recycled concrete aggregate—A review. *J. Clean. Prod.* **2016**, *112*, 466–472. [CrossRef]

38. Tam, V.W.Y.; Tam, C.M.; Le, K.N. Removal of cement mortar remains from recycled aggregate using pre-soaking approaches. *Resour. Conserv. Recycl.* **2007**, *50*, 82–101. [CrossRef]

39. Kou, S.-C.; Poon, C.-S. Properties of concrete prepared with PVA-impregnated recycled concrete aggregates. *Cem. Concr. Compos.* **2010**, *32*, 649–654. [CrossRef]

40. Kou, S.C.; Poon, C.S. Enhancing the durability properties of concrete prepared with coarse recycled aggregate. *Constr. Build. Mater.* **2012**, *35*, 69–76. [CrossRef]

41. Grabiec, A.M.; Klama, J.; Zawal, D.; Krupa, D. Modification of recycled concrete aggregate by calcium carbonate biodeposition. *Constr. Build. Mater.* **2012**, *34*, 145–150. [CrossRef]

42. Xuan, D.; Zhan, B.; Poon, C.S. Durability of recycled aggregate concrete prepared with carbonated recycled concrete aggregates. *Cem. Concr. Compos.* **2017**, *84*, 214–221. [CrossRef]

43. Gao, D.; Zhang, L.; Nokken, M. Compressive behavior of steel fiber reinforced recycled coarse aggregate concrete designed with equivalent cubic compressive strength. *Constr. Build. Mater.* **2017**, *141*, 235–244. [CrossRef]

44. Gao, D.; Zhang, L. Flexural performance and evaluation method of steel fiber reinforced recycled coarse aggregate concrete. *Constr. Build. Mater.* **2018**, *159*, 126–136. [CrossRef]

45. Carneiro, J.A.; Lima, P.R.L.; Leite, M.B.; Toledo Filho, R.D. Compressive stress–strain behavior of steel fiber reinforced-recycled aggregate concrete. *Cem. Concr. Compos.* **2014**, *46*, 65–72. [CrossRef]

46. Anike, E.E.; Saidani, M.; Olubanwo, A.O.; Tyrer, M.; Ganjian, E. Effect of mix design methods on the mechanical properties of steel fibre-reinforced concrete prepared with recycled aggregates from precast waste. *Structures* **2020**, *27*, 664–672. [CrossRef]

47. Haido, J.H. Flexural behavior of basalt fiber reinforced concrete beams: Finite element simulation with new constitutive relationships. *Structures* **2020**, *27*, 1876–1889. [CrossRef]

48. Kang, W.-H.; Ramesh, R.B.; Mirza, O.; Senaratne, S.; Tam, V.; Wigg, D. Reliability based design of RC beams with recycled aggregate and steel fibres. *Structures* **2017**, *11*, 135–145. [CrossRef]

49. Akça, K.R.; Çakır, Ö.; İpek, M. Properties of polypropylene fiber reinforced concrete using recycled aggregates. *Constr. Build. Mater.* **2015**, *98*, 620–630. [CrossRef]

50. Lee, J.-H.; Cho, B.; Choi, E.; Kim, Y.-H. Experimental study of the reinforcement effect of macro-type high strength polypropylene on the flexural capacity of concrete. *Constr. Build. Mater.* **2016**, *126*, 967–975. [CrossRef]

51. Patel, P.A.; Desai, A.K.; Desai, J.A. Evaluation of engineering properties for polypropylene fibre reinforced concrete. *Int. J. Adv. Eng. Technol.* **2012**, *3*, 42–45.

52. Kazmi, S.M.S. *Improvement of the Mechanical and Durability Performance of Recycled Aggregate Concrete*; RMIT University: Melbourne, Australia, 2020.

53. Behfarnia, K.; Behravan, A. Application of high performance polypropylene fibers in concrete lining of water tunnels. *Mater. Des.* **2014**, *55*, 274–279. [CrossRef]

54. Shen, D.; Liu, C.; Li, C.; Zhao, X.; Jiang, G. Influence of Barchip fiber length on early-age behavior and cracking resistance of concrete internally cured with super absorbent polymers. *Constr. Build. Mater.* **2019**, *214*, 219–231. [CrossRef]

55. Common Wealth Scientific Industrial Research Organization. *Guide for Specification of Recycled Concrete Aggregate for Concrete Production (H155-2002)*; Standards Australia: Sydney, Australia, 2002.

56. AS 2758.1:2014. *Aggregates and Rock for Engineering Purposes: Part 1. Concrete Aggregates*; Standards Australia: Sydney, Australia, 2014.

57. ASTM C192:2016. Standard practice for making and curing concrete test specimens in the laboratory. In *American Society of Testing and Materials*; ASTM: West Conshohocken, PA, USA, 2016.

58. Kazmi, S.M.S.; Munir, M.J.; Wu, Y.-F.; Patnaikuni, I.; Zhou, Y.; Xing, F. Influence of different treatment methods on the mechanical behavior of recycled aggregate concrete: A comparative study. *Cem. Concr. Compos.* **2019**, *104*, 103398. [CrossRef]

59. Munir, M.J.; Wu, Y.-F.; Kazmi, S.M.S.; Patnaikuni, I.; Zhou, Y.; Xing, F. Stress-strain behavior of spirally confined recycled aggregate concrete: An approach towards sustainable design. *Resour. Conserv. Recycl.* **2019**, *146*, 127–139. [CrossRef]

60. Munir, M.J.; Kazmi, S.M.S.; Wu, Y.-F.; Patnaikuni, I.; Zhou, Y.; Xing, F. Stress strain performance of steel spiral confined recycled aggregate concrete. *Cem. Concr. Compos.* **2020**, *108*, 103535. [CrossRef]

61. Munir, M.J.; Kazmi, S.M.S.; Wu, Y.-F.; Patnaikuni, I. Influence of concrete strength on the stress-strain behavior of spirally confined recycled aggregate concrete. *IOP Conf. Ser. Mater. Sci. Eng.* **2020**, *829*, 012004. [CrossRef]

62. Wei, Y.; Wu, Y.-F. Compression behavior of concrete columns confined by high strength steel wire. *Constr. Build. Mater.* **2014**, *54*, 443–453. [CrossRef]

63. Nataraja, M.C.; Dhang, N.; Gupta, A.P. Stress–strain curves for steel-fiber reinforced concrete under compression. *Cem. Concr. Compos.* **1999**, *21*, 383–390. [CrossRef]

64. Xiao, J.; Zhang, K.; Akbarnezhad, A. Variability of stress-strain relationship for recycled aggregate concrete under uniaxial compression loading. *J. Clean. Prod.* **2018**, *181*, 753–771. [CrossRef]

65. Munir, M.J.; Kazmi, S.M.S.; Wu, Y.-F.; Lin, X. Axial stress-strain performance of steel spiral confined acetic acid immersed and mechanically rubbed recycled aggregate concrete. *J. Build. Eng.* **2020**, *34*, 101891. [CrossRef]

66. Chaboki, H.R.; Ghalehnovi, M.; Karimipour, A.; de Brito, J. Experimental study on the flexural behaviour and ductility ratio of steel fibres coarse recycled aggregate concrete beams. *Constr. Build. Mater.* **2018**, *186*, 400–422. [CrossRef]

67. Li, V.C. A simplified micromechanical model of compressive strength of fiber-reinforced cementitious composites. *Cem. Concr. Compos.* **1992**, *14*, 131–141. [CrossRef]

68. Kou, S.-C.; Poon, C.-S.; Wan, H.-W. Properties of concrete prepared with low-grade recycled aggregates. *Constr. Build. Mater.* **2012**, *36*, 881–889. [CrossRef]

69. Liu, Y.; Wang, W.; Chen, Y.F.; Ji, H. Residual stress-strain relationship for thermal insulation concrete with recycled aggregate after high temperature exposure. *Constr. Build. Mater.* **2016**, *129*, 37–47. [CrossRef]

70. Xiao, J.; Li, J.; Zhang, C. Mechanical properties of recycled aggregate concrete under uniaxial loading. *Cem. Concr. Res.* **2005**, *35*, 1187–1194. [CrossRef]

71. Counto, U.J. The effect of the elastic modulus of the aggregate on the elastic modulus, creep and creep recovery of concrete. *Mag. Concr. Res.* **1964**, *16*, 129–138. [CrossRef]

72. Suksawang, N.; Wtaife, S.; Alsabbagh, A. Evaluation of elastic modulus of fiber-reinforced concrete. *ACI Mater. J.* **2018**, *115*, 239–249. [CrossRef]

73. Nematzadeh, M.; Baradaran-Nasiri, A. Residual properties of concrete containing recycled refractory brick aggregate at elevated temperatures. *J. Mater. Civ. Eng.* **2018**, *30*. [CrossRef]

74. Taerwe, L.R. Influence of steel fibers on strain-softening of high-strength concrete. *Mater. J.* **1993**, *89*, 54–60.

75. Poon, C.S.; Shui, Z.H.; Lam, L. Compressive behavior of fiber reinforced high-performance concrete subjected to elevated temperatures. *Cem. Concr. Res.* **2004**, *34*, 2215–2222. [CrossRef]

76. Topçu, İ.B.; Canbaz, M. Effect of different fibers on the mechanical properties of concrete containing fly ash. *Constr. Build. Mater.* **2007**, *21*, 1486–1491. [CrossRef]